MEMS HYDRODYNAMIC BEARINGS: APPLICATIONS AND IMPLICATIONS TO MACHINE-FAILURE PREVENTION

Kristin L. Wood, Dean Neikirk, Ilene Busch-Vishniac, William Weldon, Chin-Seng Chu, Youndmin Kim, Vikas Gupta, William Maddox, and David Masser

Departments of Mechanical and Electrical Engineering
The University of Texas, Austin, TX 78712

Abstract: Microdynamical systems have been studied for a number of years. Only limited work, however, has been completed on integrating microdynamical components into systems that satisfy mechanical tasks on *macroscopic* scales. In this paper, we describe microdynamical components that are needed to produce a surface which is actively deformable on local scales. In particular, we consider the design and demonstration of smart journal and thrust bearings capable of using embedded sensors and actuators to dynamically change the surface geometry. The ability to actively deform bearing surfaces allows for the design of bearings which are less prone to failure, the design of bearings with greater load carrying abilities, and a fundamental study of the effect of surface geometries and fluid conditions on bearing performance, such as start-up and shut-down conditions. Results of our new bearing designs are presented, focusing on numerical bearing models, sensor and actuator design and fabrication, and physical experimentation.

Key Words: Hydrodynamic bearings; new technology; micro-electro-mechanical systems (MEMS); steady-state and dynamic analysis; turbomachinery

INTRODUCTION: Bearings are low-level devices that perform a wide variety of functions within higher-level systems, e.g., motors, engines, pumps, and turbines. These functions, such as support load, guide motion, and attenuate dynamic conditions, are usually critical to the higher-level system's performance and reliability. As a result, unsatisfactory bearing design or poor bearing selection can be devastating to the system's life cycle and maintenance. Despite current efforts to limit these circumstances, increasingly exotic high-level systems are encroaching on the technical limitations of conventional bearing designs (Bhat, 1982). A novel bearing design, implementing micro-electro-mechanical systems technology, is presented to address this need.

Role of Smart Bearing: Smart bearings offer a possible solution to the failure of conventional bearing styles. For the sake of definition, a smart bearing is a system that senses and adapts to instantaneous operating conditions by varying a design parameter (such as clearance in the case of a hydrodynamic foil bearing) or by exploiting one or more physical parameters (such as ferromagnetism in the case of an active magnetic bearing) (Ku, 1990; Siegwart, 1991). In essence, the bearing's design and/or control features possess the capability to sense instantaneous system stimuli and respond accordingly. These capabilities suggest that a smart bearing could control the performance of the overall rotor-bearing system. Since bearing design parameters and performance parameters are inherently coupled, the dynamic and static characteristics of a rotor-bearing system could be actively controlled. In turn, critical mode vibrations could be attenuated if the bearing could sense system conditions and actuate an appropriate bearing clearance. In the next section, we present a new smart bearing concept, designed specifically to address both dynamic and static performance issues.

MEMS SMART BEARING CONCEPT: Geometric design parameters have an effect on the performance of hydrodynamic bearing systems. These variations in geometric form

could be accommodated through macroscopic or microscopic methods of actuation and sensory control. This research effort explores the possibility of implementing microscopic devices in the role of sensors and actuators. The choice of micro over macro is based upon the recent advancements of VLSI manufacturing technology -- which have also lead to the sudden proliferation of integrable microelectromechanical devices. Such an integrated system could reduce or eliminate the need for external actuator and sensory devices. This advantage saves space and required power, while increasing the possibilities of local fluid control.

Studies suggest that hydrodynamic performance can be affected by microscopic variations in the bearing surface profile (Tzeng, 1991; Hargreaves, 1991, Srinivasin, 1995). This knowledge leads to the development of a hydrodynamic slider bearing with an actively deformable surface. An example of this smart bearing concept is illustrated in Figure 1. An actively deformable surface is defined as a surface that undergoes microscopic variations to achieve a desired profile or layout (Maddox, 1994). These surfaces are composed of an array of micron-scale sensors and actuators. A possible layout of such an array is illustrated in Figure 2.

MEMs surfaces can operate on global or local surface characteristics. In global surface control, an overall surface structure is actively prescribed by a central processor. Hypothetically, an array of pressure data could be collected from a slider bearing surface. Upon processing, the pressure profile could be modified by actively deforming the bearing from a flat to a crowned surface. In local surface control, sensing, control, and actuation are accomplished locally in order to produce either a purely local or a global effect. The surface is composed of *cellular automata*, where all necessary operations are carried out within each individual cell or a cell and its nearest neighbors, thus avoiding the difficulties of global interconnections. In such a system, local control could be used to minimize local pressure gradients across a slider bearing surface which, in turn, could globally affect the bearing's instantaneous load capacity.

Because of the potential advantages of local surface control, this research concentrates on creating microscale surface deformations on slider bearing surfaces to produce macroscale performance variations. The ability to actively deform bearing surfaces will allow for the design of bearings which may control one or more of the following performance characteristics: stiffness, damping, load capacity, power loss, cavitation, film thickness, clearance, etc.

MICROFABRICATION AND MEMS: To create the deformable surfaces discussed above, micromachining techniques must be employed to produce the microdevices which comprise the surface. This section discusses the various surface features and sensors being developed for use in a smart bearing.

Surface Features: Based on the micromachining techniques that presently exist, two types of surface features are being investigated. Membrane surface features are diaphragm-type actuators which deform due to an applied pressure. The other type of surface features are fixed features, which are permanently etched into a silicon wafer.

To create the membrane features, alternating layers of silicon oxide and silicon nitride are deposited onto a silicon wafer using low pressure chemical vapor deposition (LPCVD). Typical individual layer thicknesses range from 0.5 μm to 2 μm. Next, the silicon wafer is back-etched to release rectangular sections of the dielectric films. The film sections released by the back etching process are the membranes which deform due to the applied pressure. To form the fixed features, a mask is deposited on the wafer surface to prevent undesired etching of the silicon wafer. An anisotropic etchant is then used to remove the unwanted silicon, controlling feature depth with careful timing.

Individual membrane and fixed features are combined to form membrane surfaces, fixed surfaces, or hybrid (combined membrane and fixed) surfaces. The overall surface and feature dimensions are constrained based upon the crystallographic orientation of the silicon wafers, the silicon wafer

thickness, the feature type, whether the feature is adjacent to the surface edge, and the type of adjacent features. These constraints are due to limitations in the micromachining processes. For example, if two membrane features are placed adjacent to one another on a (110) silicon wafer, the features must be placed at least 10 microns apart. This constraint is due to the minimum required bonding distance for the silicon wafer.

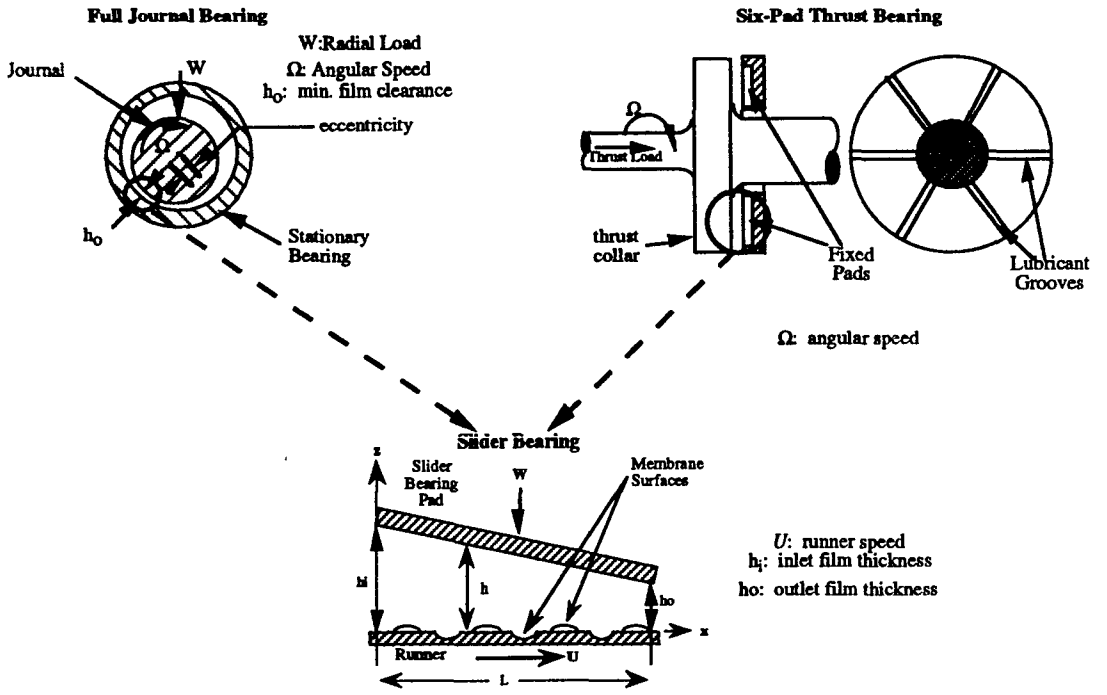

Note: the regions encircled on the journal and thrust bearings can be approximated by a slider bearing

Figure 1. Side view of a smart slider bearing approximation with a deformable surface.

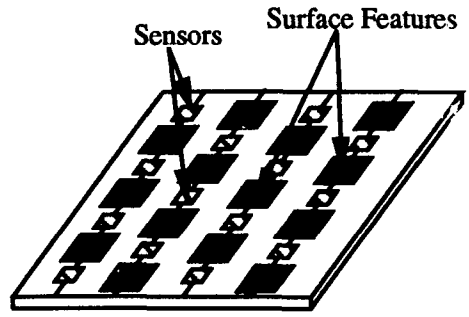

Figure 2. Planar view of an actively deformable surface with embedded sensors.

Sensors — Modeling and Fabrication: Besides the general surface design and fabrication, our work on sensors and actuators for active bearings has focused on a pressure sensor, which uses an optical transduction method, and a proximity sensor, which uses an inductive transduction approach. Each of these sensors is briefly described below.

Fabry-Perot Based Pressure Transducers: Microsensors embedded in a bearing surface should allow localized measurements, for example pressure and temperature, without disturbing the measurand. The local measurements will determine dynamic characteristics of the bearing fluid film and verify a model for bearing performance. The microsensor for pressure measurement is implemented using optical interferometry. Pressure applied to the membrane is measured by detecting the deflection of the membrane. Advantages of optical measurement are as follows: remote data acquisition is achieved without loss of signal to noise ratio, pressure averaging effect reducing sensitivity of piezoresistive pressure sensor is avoided, and dimensions of the device could be much smaller than capacitive pressure sensor.

The Fabry-Perot cavity and optical fiber are used as the sensing element and interconnect, respectively. The cavity is monolithically built by etching a sacrificial layer that lies between dielectric film stacks. The gap of the cavity can be precisely adjusted by controlling the thickness of a sacrificial layer grown using LPCVD. With LPCVD, multiple dielectric films (consisting of silicon dioxide and silicon nitride) can be deposited to form wavelength selective dielectric mirrors. The technique allows for batch fabrication of the pressure sensors with excellent alignment and parallelism of the two mirrors in the cavity.

Fabry-Perot cavity-based sensors have been widely used for their versatility; for example they have been used to sense both pressure and temperature (Halg, 1992; Dakin, 1987; Lee, 1991; Wolthuis, 1991). This kind of sensor detects changes in optical path length induced by either a change in the refractive index or a change in physical length of the cavity. Micromachining techniques make Fabry-Perot sensors more attractive by reducing the size and the cost of the sensing element. Another advantage of the miniature Fabry-Perot sensor is that low coherence light sources, such as light emitting diodes (LEDs), can be used to generate the interferometric signal, since the optical length of the miniature cavity is of the same order as the wavelength of the light.

In these devices, the cavity mirrors can be either dielectric layers or metal layers deposited or evaporated during the manufacturing process. The thickness of each layer must be tightly controlled to achieve the target performance of a sensor. However, there are unavoidable errors in thickness even though techniques of thickness control for thin films have rapidly improved (Macleod, 1986). For Fabry-Perot optical interference filters, it has long been recognized that the performance of the filter is greatly influenced by random thickness variations in the films used (Bousquet, 1972; Macleod, 1976). For instance, the resonant wavelength is very sensitive to thickness variations. We have considered the impact of manufacturing errors on the performance of such sensors. In particular, we have considered how random errors in thickness of the cavity mirrors influence the accuracy with which gap can be measured. We have found that an optimum combination of initial gap and mechanical travel of the cavity exists for a given mirror design which gives the least variation in response curve (Kim, 1994).

Proximity Sensors: One of the most difficult quantities to monitor in a bearing is the actual gap between the bearing pad and the runner. Previous work (Grover, 1929) suggests the use of inductive sensing techniques (eddy current sensors); our current bearing tester uses commercially available proximity sensors mounted externally to the silicon bearing pad. An initial calibration procedure with the runner fixed must be used to locate the reference plane of the sensors with respect to the actual pad location, leading to one of the most significant potential sources of error in the actual bearing gap determination.

To act as the transducer for an *in-situ* proximity sensor, a planar inductor is fabricated directly on the silicon bearing pad. Models developed by Grover (Grover 1929; Grover, 1962) and Greenhouse (1974) are used to calculate the inductance of different planar coil configurations. Experiments to validate these models of a variable gap between the coils and an electrically "floating" plate have been performed. The experiments and model show that there is a decrease in the inductance of the total system (coil and plate) as the gap between the coil and plate decreases.

This is due to the increase in the mutual inductance between the plate and the coil. Different coil configurations show a different amount of absolute inductance change for the same gap. This result indicates that the rectangular spiral may be the best design choice.

A configuration using two coils, forming a planar transformer, has been explored as an alternative to the conventional single-coil sensor. With this arrangement, the gain and the phase of the output changes as the plate gap decreases. Using Grover's (1962) and Greenhouse's (1974) model, values for the inductance of the coils have been calculated. Using these values, a SPICE model for the planar transformer has also been developed. The twin coil design avoids the problem of low Q in planar, small geometry spiral inductors. By measuring a phase difference between input and output coils, the operating frequency remains largely insensitive to the resistance of the transducer, which is critical in "miniaturized" IC inductors.

BEARING MODELS AND EXPERIMENTS: Using the MEMs surfaces and devices introduced above, the goal of this section is to demonstrate performance results of bearing modeling and experimentation. This section first presents the relevant steady state modeling results, followed by experimentation and dynamic modeling.

Steady State Modeling: To determine the performance parameters of a hydrodynamic bearing, fluid flow models based upon hydrodynamic lubrication theory are needed. The relevant hydrodynamic lubrication theory for a slider bearing is the normalized Reynolds' Equation:

$$\frac{\partial}{\partial \bar{x}}\left(\bar{h}^3 \frac{\partial \bar{p}}{\partial \bar{x}}\right)+\left(\frac{L}{B}\right)^2 \frac{\partial}{\partial \bar{y}}\left(\bar{h}^3 \frac{\partial \bar{p}}{\partial \bar{y}}\right)=6\frac{\partial \bar{h}}{\partial \bar{x}} \qquad (1)$$

where L and B is the bearing length and breadth, respectively, and the normalized film thickness equation is:

$$\bar{h}(\bar{x},\bar{y}) = H_x - (H_x - 1)\bar{x} - \bar{w}(\bar{x},\bar{y}) \qquad (2)$$

where H_X is the inlet to outlet height ratio. Reynolds' Equation is then solved numerically using successive over-relaxation (SOR). Due to the converging and diverging geometry of the surface features, the Reynolds' boundary condition is incorporated to form the rupture and reformation boundaries for any predicted cavitation regions (Hargreaves, 1991).

Based upon the lubricant pressure profile determined from Equation 1, performance parameters are calculated to determine the performance ranges of the smart bearing system. Examples of relevant performance parameters are the load capacity, friction force, flow rates.

Using these performance parameters, the operating ranges for the membrane and fixed bearing surfaces may be determined. To facilitate the design of membrane, fixed feature, and hybrid surfaces, surface parameters are developed (Maddox, 1994). The surface design parameters provide an efficient means of conveying the necessary design information of the individual features while describing the overall surface geometry. A major benefit of the surface design parameters is the ability to exchange information in an efficient manner between surface designers, modelers, and manufacturers. Another benefit is the ability to vary individual surface design parameters to determine the individual effects on bearing performance.

The surface design parameters are analyzed using a factorial design (Maddox, 1994). A factorial design is implemented due to its efficiency and ability to determine variable (surface parameter) interactions (Hicks, 1982).. While many design rules and inferences have been made with regard to the steady-state modeling, some of the significant results are given below (Maddox, 1994):

- With the membrane surfaces, the load capacity varies from -30 to 110% from the nominal smooth surface bearing.
- A low number (five) of membrane features are adequate for altering the performance characteristics. In fact, no significant variation occurs by adding additional features.
- Fixed features can alter the load capacity by 20 to 100% from the nominal smooth surface bearing.
- Hybrid features can alter the load capacity form -32 to 53% from the nominal smooth surface bearing.

The modeling results demonstrate that the MEMs surfaces can be used to alter bearing clearances, vary the bearing stability, and correct for wear within the bearing (Maddox, 1994). Thus, the MEMs surfaces should be useful in making a hydrodynamic bearing relatively insensitive to internal parameter variations and external disturbances.

Experimental Apparatus: The basic platform for the test apparatus consists of a Harig model 618 surface grinder. The grinder provides a rotating bearing surface, fluid delivery system and precise three axis translation, a novel approach compared to other *scaled-up* bearing experimental experiments (Hargreaves, 1991). A custom subassembly shown in Figures 3 and 4 is designed to provide rotational orientation and the measurement instrumentation required of the bearing.

The bearing subassembly manifold, instrumentation, and orientation systems have been built and assembled as a unit and are mounted to the grinder. These systems provide two rotational degrees of adjustment; mounting ports for up to four micrometer heads and four eddy-current proximity sensors; sixteen sealed airlines; and force measurement in the thrust and drag directions. The rotational degrees of freedom are used to achieve proper initial orientation of the stationary (non-rotating) bearing surface as well as to help compensate for any deflections due to loading.

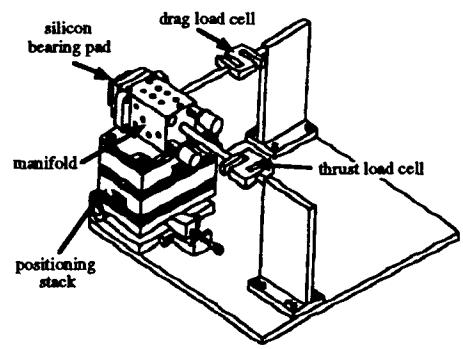

Figure 3 Detailed drawing of thrust bearing subassembly.

Wedge drive screws and wedges are designed to provide control of the apparatus as well as a useful range of motion. To restrict unwanted motion while allowing thrust and drag forces to be transmitted to the load cells, two single-axis crossed roller bearing tables are included in the system. In addition, two load cells anchor the manifold and prevent it from moving and altering the geometry of the bearing gap. Since these cells are the only structures preventing motion in the horizontal plane, they measure the thrust and drag forces acting on the bearing.

Measurement of the bearing gap is a particularly difficult task. The current manifold includes three commercially available eddy current proximity sensors. To calibrate these sensors, a bearing pad is first attached to the manifold, and the whole assembly placed in direct contact with the (non-

rotating) grinder wheel, i.e., the runner. Readings from the three proximity sensors establish the "zero gap" position of the bearing pad/manifold assembly relative to the runner surface. During actual operation, the noncontact eddy current sensors measure the position of the manifold assembly relative to this zero.

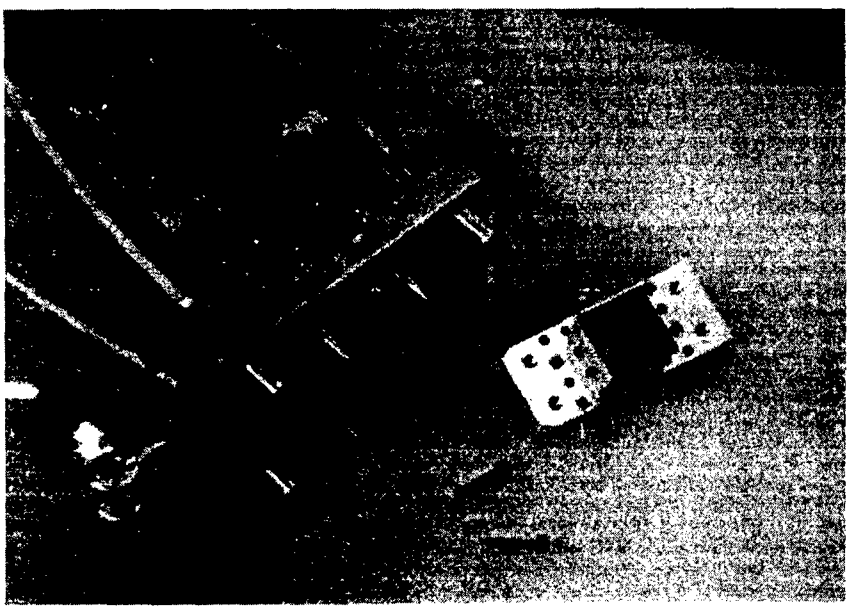

Figure 4: Photo of manifold assembly used to test micromachined bearing pads; bearing pad (fixed features) shown center-right.

Using the experimental apparatus described above, a number of bearing surfaces have been tested, with the objective to match, within experimental uncertainty, the results obtained computationally (Maddox, 1994). For example, Figure 5 shows the experimental tests obtained for a flat silicon surface and a (100) fixed featured surface at a constant angle of attack. The trends shown in Figure 5 closely follow the trends the computational results. These data indicate that loads can be varied significantly for featured bearing surfaces and for different feature depths.

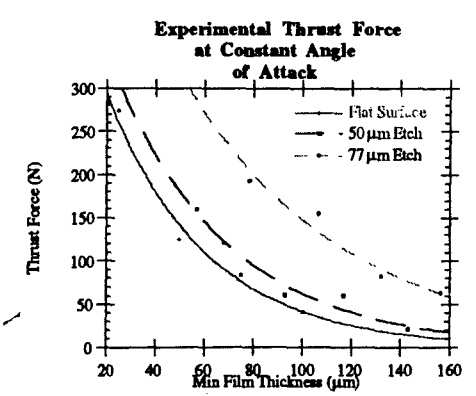

Figure 5: Load versus Film Thickness for Experimental Slider Bearing.

Dynamic Modeling: Steady state slider bearing results in the previous sections show that the presence of MEMs features in the bearing gap greatly affect bearing load, friction, and flow rates. These results also suggest possible dynamic characteristic variations due to the MEMs features (Maddox, 1994). To confirm the dynamic changes within the bearing, two dynamic issues are considered important to the practicality of smart MEMs bearings:

(1) effects of MEMs features on dynamic performance of fluid film bearings; and
(2) dynamic response of MEMs bearings under actual operating conditions.

These issues can be addressed with prior knowledge of the MEMs bearing dynamic characteristics. Consequently, the current modeling effort is focused on developing quasi-static dynamic models to calculate the stiffness and damping coefficients for the MEMs slider bearing. The remainder of this section details these dynamic modeling efforts.

Observations from an error analysis suggest the importance of higher order effects in bearing dynamic characteristics. As a result, a nonlinear dynamic model is developed to predict MEMs bearing dynamic characteristics (Chu, 1995). This model will allow bearing reaction expansion up to the desirable order of accuracy (Chu, 1995).

Analysis of dynamic model suggests that a fourth order model will produce accurate results up to a vertical displacement (Δz) of ± 0.3 times the minimum gap about a quasi-static position. Using this criterion, a fourth order dynamic model is applied to a bearing surface with four membrane features. Within the valid motion ranges ($\Delta z = \pm 0.3$ x minimum gap), comparisons between MEMs bearings and conventional bearings give the results shown in Table 1. Several conclusions may be drawn from these results:

- Within the valid motion ranges, MEMs bearings can increase the load capacity, stiffness, and damping (43 to 89%, 23 to 132%, and 0 to 66% respectively) of a conventional slider bearing with a similar configuration.
- Within the valid motion ranges, MEMs bearings can also lower the load capacity, stiffness, and damping (-18 to -58%, -21 to -60%, and -20 to -28% respectively) of a conventional slider bearing with a similar configuration.
- Actuation of membrane into the oil film especially near the location of maximum pressure will significantly increase bearing stiffness and damping.
- Actuation of membrane out of the gap will lower bearing load, bearing stiffness, and bearing damping.

Actuation Profile	Load Capacity	Stiffness	Damping
All Up	43 - 85% Higher	23 - 132% Higher	23 - 66% Higher
All Down	18 - 23% Lower	21 - 27% Lower	20 - 28% Lower
2 up, 1 flat, 2 down	54 - 58% Lower	50 - 60% Lower	Negligible Change
2 down, 1 flat, 2 up	71 - 89% Higher	55 - 112% Higher	0 - 18% Higher

Table 1. Load capacity, stiffness, and damping variations for four membrane profiles.

The dynamic model discussed in this section shows that an actively-deformable bearing has the potential for fine-level dynamic control. This characteristic of an active MEMs bearing has important implications in practice. In general, the dynamic characteristics of fluid film bearings govern the threshold for the onset of critical speeds and self excited whirl instabilities, rotor stability during operations, and rotor response to transients and external loading (Someya, 1989). Active MEMs bearings will have the ability to influence these dynamic conditions. Other applications might be maintaining clearance and correcting misalignment within the bearing pad.

CONCLUSIONS AND IMPLICATIONS: Mechanical machine components are the building blocks for automation. Perhaps the most prolific class of machine components is bearings. In this paper, a new concept is presented for hydrodynamic bearings based on MEMs technology. Fabrication approaches and results are shown for fixed and membrane surface features (actuators), for Fabry-Perot pressure sensors, and for inductive transducer sensors. These MEMs devices form the necessary components for an actively deformable surface. Modeling results of such surfaces show that bearing load carrying capacity, stiffness, and damping can all be changed by over 100%, compared to a nominal bearing configuration. Experimental results of fixed-feature surfaces support these results. Future work for this research will concentrate on further experimentation, on developing local small-scale power supplies for the sensors and actuators (Koeneman, 1995), and on system integration.

Acknowledgments: The research reported in this document was made possible in part by a grant from the Advanced Research Projects Agency (ARPA), Embedded Microsystems Program, Contract No. DABT63-92-C-0027. Any opinions, findings, conclusions, or recommendations are those of the authors and do not necessarily reflect the views of the sponsors.

REFERENCES:

Bhat, B. N. and Dolan, F. J. "Past Performance Analysis of HPOTP Bearings". NASA TM-82470, 1982.

Bousquet, P., A. Fornier, R. Kowalczyk, E. Pelletier, and P. Roche, "Optical filters: monitoring process allowing the auto-correction of thickness errors," *Thin Solid Films*, vol. 13, pp. 285 - 290, 1972.

Chu, C. S., "Dynamic Modeling of a Smart Hydrodynamic Bearing," Master's Thesis, The University of Texas, Dept. of Mechanical Engineering, Austin, TX 78712, 1995.

Dakin, J. P., C. A. Wade, and P. B. Withers, "An optical fiber pressure sensor," *SPIE Fiber optics '87:Fifth International Conference on Fiber optics and Opto-electronics*, vol. 734, pp. 194 - 201, 1987.

Greenhouse, H. M. "Design of Planar Rectangular Microelectronic Inductors," *IEEE Transactions on Parts, Hybrids, and Packaging*, vol. Vol. PHP-10, 1974.

Grover, F. W. "The Calculation of the Inductance of Single-Layer Coils and Spirals Wound with Wire of Large Cross Section," *Proceedings of the Institute of Radio Engineers*, vol. 17, pp. 2053-2063, 1929.

Grover, F. W. *Inductance Calculations, Working Formulas and Tables.* New York: Dover, 1962.

Gu, A. "Process Fluid Foil Bearing Liquid Hydrogen Turbopump". AIAA Document 88-3130, 1988..

Halg, B. "A silicon pressure sensor with a low-cost contactless interferometric optical readout," *Sensors and Actuators A*, vol. 30, pp. 225- 229, 1992.

Hamrock, B. J. *Fundamental of Fluid Film Lubrication.* McGraw-Hill,New York, 1994. Pages 244-252.

Hargreaves, D. J. "Surface Waviness Effects on the Load-Carrying Capacity of Rectangular Slider Bearings". *Wear*, vol. 145, pp. 137-151, 1991.

Heshmat, H. "Smart Bearing Boosts Air Turbine Efficiency". *Design News*. pp. 101-102, 1993.

Hicks, C. R. *Fundamental Concepts in the Design of Experiments*. Holt, Rinehart, and Winston. New York, 3rd ed, 1982.

Kim, Y. and D. P. Neikirk, "Design for Manufacture of Micro Fabry-Perot Cavity-based Sensors," *submitted to Sensors and Actuators A*, 1994.

Koeneman, P., "Conceptual Design of a Micro Power Supply," Master's Thesis, The University of Texas, Dept. of Mechanical Engineering, Austin, TX 78712, 1995.

Ku, C.-P. R. and Heshmat, H. "Compliant Foil Bearing Structural Stiffness Analysis: Part I -- Theoretical Model Including Strip and Variable Bump Foil Geometry". *Journal of Tribology, Transactions of the ASME*, vol. 114, pp. 394-400, 1990.

Lee, C. E. and H. F. Talyor, "Fiber-optic Fabry-Perot Temperature Sensor Using a Low-Coherence Light Source," *Journal of Lightwave Technology*, vol. 9, pp. 129 - 134, 1991.

Lund, J. W. " Review of the Concept of Dynamic Coefficients for Fluid Film Journal Bearings". Journal of Tribology, 109:37-41, 1987.

Macleod, H.A. "Thin film narrow band optical filters," *Thin Solid Films*, vol. 34, pp. 335 - 342, 1976.

Macleod, H. A. *Thin-film optical filters*. New York: McGraw-Hill, 1986.

Maddox, W. E. "Modeling and Design of a Smart Hydrodynamic Bearing with an Actively Deformable Surface". Master's Thesis, The University of Texas at Austin. Austin, Texas, 1994.

Nagaya, K. and S. Takeda. "Active Control Method for passing Through Critical Speeds of Rotating Shafts by Changing Stiffness of the Supports with Use of Memory Metals". Journal of Sound and Vibration, 113(2):307-315, 1987.

Siegwart R. and Truninger, R. "Electromagnetic Bearings, a Resonable Element in Turbomachinery?". *Rotating Machinery Dynamics, Proceedings of the Third International Symposium on Transport Phenomena and Dynamics of Rotating Machinery*. pp. 253-267, 1991.

Someya, T. *Journal-Bearing Databook*. Springer-Verlag, Germany, 1989. Pages 288-294.

Srinivasan, R. S. and Wood, K. L. "Geometric Tolerancing for Mechanical Design Using Fractal-Based Parameters". *ASME Journal of Mechanical Design*, vol. 117, no. 1, pp. 203-205, 1995.

Tabata, O., K. Shimaoka, and S. Sugiyama, "In Situ Observation and Analysis of wet etching process for Microelectromechanical Systems," *Proc. IEEE Workshop on Microelectromechanical Systems*, 1991, pp. 99-102.

Tzeng, S. T. and Saibel, E. "Surface Roughness Effect on Slider Bearing Lubrication". *ASLE Transactions*, vol. 10, pp. 334-338.

Wolthuis, R.A., G. L. Mitchell, E. Saaski, J. C. Hartl, and M. A. Afromowitz, "Development of medical pressure and temperature sensors employing optical spectrum modulation," *IEEE Trans. on Biomedical Engin.*, vol. 38, pp. 974 - 980, 1991.